Variant of Human Enzyme Sequesters Reactive Intermediate†

Karla L. Ewalt,* Xiang-Lei Yang, Francella J. Otero, Jianming Liu, Bonnie Slike, and Paul Schimmel

Skaggs Institute for Chemical Biology, The Scripps Research Institute, 10550 North Torrey Pines Road, Mail Drop BCC-379, La Jolla, California 92037

Received September 1, 2004; Revised Manuscript Received January 13, 2005

ABSTRACT: In cellular environments, coupled hydrolytic reactions are used to force efficient product formation in enzyme-catalyzed reactions. In the first step of protein synthesis, aminoacyl-tRNA synthetases react with amino acid and ATP to form an enzyme-bound adenylate that, in the next step, reacts with tRNA to form aminoacyl-tRNA. The reaction liberates pyrophosphate (PP_i) which, in turn, can be hydrolyzed by pyrophosphatase to drive efficient aminoacylation. A potential polymorphic variant of human tryptophanyl-tRNA synthetase is shown here to sequester tryptophanyl adenylate. The bound adenylate does not react efficiently with the liberated PP_i that normally competes with tRNA to resynthesize ATP and free amino acid. Structural analysis of this variant showed that residues needed for binding ATP phosphates and thus PP_i were reoriented from their conformations in the structure of the more common sequence variant. Significantly, the reorientation does not affect reaction with tRNA, so that efficient aminoacylation is achieved.

As a group, aminoacyl-tRNA synthetases are among the most ancient proteins and are thought to have evolved during the transition from the RNA world to the protein world. They catalyze fundamental reactions that pair amino acids with their cognate tRNAs for ribosomal protein synthesis. In the first step of protein synthesis, aminoacyl-tRNA synthetases react with amino acid and ATP to form an enzyme-bound aminoacyl adenylate. That reaction liberates pyrophosphate (PP_i),[1] which in turn is hydrolyzed by pyrophosphatase to drive efficient aminoacylation. In the second step, the activated amino acid subsequently reacts with tRNA to yield aminoacyl-tRNA. The two steps in the reaction are chemically independent, but in some enzymes, such as GlnRS, aminoacyl-AMP formation requires that cognate tRNA is simultaneously bound to the enzyme (*1*).

Consistent with the high and competing (with respect to tRNA) reactivity of PP_i, the overall aminoacylation reaction is much more efficient in the presence of pyrophosphatase (*2*). Indeed, pyrophosphatases in general provide a powerful stimulus to nucleotide triphosphate-driven reactions. Here we present a variant of a tRNA synthetase that has a significantly reduced activity with PP_i, thus reducing the reverse reaction in favor of aminoacylation.

The 10 class I tRNA synthetases have been categorized into one of three subclasses, based on sequence similarities (*3*, *4*). Two enzymes are grouped together in subclass Ic, TrpRS and TyrRS. Both are obligate homodimers that are superposable in the core catalytic regions (*5*, *6*). Structural comparison of the active sites and Rossmann-fold domains of *Bacillus stearothermophilus* TrpRS and *B. stearothermophilus* TyrRS (*5*) showed that the backbone carbons overlapped with an rms deviation of 1.69 Å. Phylogenetic analyses indicated a close relationship between TrpRS and TyrRS (*6*−*8*).

B. stearothermophilus TyrRS has been one of the most extensively investigated aminoacyl-tRNA synthetases. Particularly with respect to understanding catalysis, more is known about this aminoacyl-tRNA synthetase than all others (*9*−*14*). Crystal structures of free, ATP-bound, Trp-bound, ATP- and tryptophanamide-bound, and Trp-AMP-bound TrpRS clearly illustrated the residues involved in binding the ligands and enclosing the active site (*15*). Due to the close relationship between TyrRS and TrpRS, many of the catalytic principles learned from the studies on *B. stearothermophilus* TyrRS are applied to TrpRS. Both are believed to follow the random, bi-bi kinetic scheme that was originally worked out for *B. stearothermophilus* TyrRS (*15*).

Here we compare the enzymatic properties of two sequence variants of human TrpRS. We also compare the crystal structure of one variant that contained a stable, naturally formed aminoacyl-AMP in the active site (*6*) to the structure of the other variant (*16*). These comparisons supported the idea that one of the sequence variants confines bound aminoacyl-AMP in its active site. Extensive kinetic data show that, indeed, the naturally formed Trp-AMP reacts rapidly with tRNA and, at the same time, has significantly reduced reactivity with PP_i. In contrast, for the other variant, Trp-AMP reacted rapidly with both PP_i and tRNA.

EXPERIMENTAL PROCEDURES

Construction of TrpRS Sequence Variants. The gene encoding human TrpRS was cloned from a human leukocyte library into a pET20b expression vector to give plasmid pFJO047. This clone encoded amino acids $S^{213}Y^{214}$. A variant

† This work was supported by Grant GM 15539 from the National Institutes of Health and by a fellowship from the National Foundation for Cancer Research.

* Corresponding author: (858) 784-8970 (phone); (858) 784-8990 (fax); kewalt@scripps.edu (e-mail).

[1] Abbreviations: TrpRS, tryptophanyl-tRNA synthetase; TyrRS, tyrosyl-tRNA synthetase; PP_i, pyrophosphate.

10.1021/bi048116l CCC: $30.25
Published on Web 02/23/2005

containing $G^{213}D^{214}$ was prepared by site-directed mutagenesis using the QuikChange mutagenesis kit to give plasmid pBMS508. Single point mutants were produced by mutagenesis of pFJO047.

Protein Expression and Purification. Human TrpRS variants fused to a C-terminal His_6 tag were expressed from pET20b plasmids in *Escherichia coli* strain BL21(DE3). Cultures were grown in Luria broth at 37 °C to mid-log phase and induced with 1 mM isopropyl β-D-thiogalactopyranoside (IPTG) for 4 h. Cells were collected by centrifugation, lysed with a French press, and clarified by ultracentrifugation at 110000*g*. TrpRS variants were purified from the soluble fraction by Ni-NTA affinity chromatography as follows. The soluble fraction was diluted in wash buffer (20 mM Tris-HCl, pH 7.9, 30 mM imidazole, 500 mM sodium chloride) and loaded onto a column of Ni-NTA agarose. The column was washed and eluted with a linear gradient of 30−250 mM imidazole in 20 mM Tris-HCl, pH 7.9, and 500 mM sodium chloride. Fractions containing protein were pooled and concentrated in a Centricon Centriprep-10. For enzymatic studies, the protein was dialyzed sequentially against phosphate-buffered saline and 50% glycerol in phosphate-buffered saline with 5 mM β-mercaptoethanol.

Enzymatic Assays. TrpRS variants were tested in aminoacylation or PP_i exchange assays at the same active site concentration (*17*). TrpRS(GD) TrpRS(SD), for which active site concentrations could not be measured due to low activity, were used at the same protein concentration as TrpRS(SY). Aminoacylation reactions were performed at 150 mM Hepes, pH 7.4, 150 mM potassium chloride, 15 mM magnesium acetate, 3 mM ATP, 3 μM [^{3}H]tryptophan, 2.5 mM dithiothreitol, and 10 μM bovine $tRNA^{Trp}$ transcript or 200 μM bulk yeast tRNA. Aminoacylation reactions were initiated by the addition of 3.5 nM enzyme and performed at 37 °C. Samples were collected at various times and spotted onto Whatman filter disks previously soaked with 0.2% tryptophan in 5% trichloroacetic acid and dried. The filters were washed three times with 5% trichloroacetic acid and twice with ethanol before scintillation counting.

PP_i exchange reactions were performed at 100 mM Tris-HCl, pH 7.8, 10 mM potassium fluoride, 2 mM magnesium chloride, 1 mM ATP, 2 or 10 mM sodium pyrophosphate or sodium [^{32}P]pyrophosphate, 2 mM tryptophan, and 5 mM β-mercaptoethanol. Reactions were initiated by the addition of 0.2 μM enzyme and carried out at room temperature. At each time point, samples were quenched in 4% charcoal, 11% perchloric acid, 200 mM sodium pyrophosphate, and 2 mM tryptophan. The charcoal was collected and washed once with 1% perchloric acid and 200 mM sodium pyrophosphate prior to scintillation counting.

Gel Filtration Chromatography. Enzyme−Trp-AMP complexes were formed under two conditions for purification by gel filtration. PP_i-containing reactions mimicked those used during PP_i exchange reactions with 5 μM TrpRS(GD) or TrpRS(SY) incubated in a buffer containing 1 mM ATP, 2 mM PP_i, and 20 μM [^{3}H]tryptophan in 150 mM Hepes, pH 7.5, 15 mM MgOAc, 150 mM KCl, and 2.5 mM DTT at 37 °C for 70 min. The other condition mimicked aminoacylation reactions but lacked tRNA. TrpRS(GD) or TrpRS(SY) (5 μM) was incubated with 3 mM ATP and 20 μM [^{3}H]tryptophan in 150 mM Hepes, pH 7.5, 15 mM MgOAc, 150 mM KCl, and 2.5 mM DTT at 37 °C for 10 min. The reaction mixtures (200 μL) were loaded onto a Superdex 200 column and eluted in 150 mM Hepes, pH 7.5, 15 mM MgOAc, and 150 mM KCl. Portions of each fraction were subjected to scintillation counting. Fractions containing the enzyme−Trp-AMP complex were pooled for further analysis in aminoacylation reactions or rechromatographed on the gel filtration column. Single turnover charging reactions were performed by adding 200 μM bulk yeast tRNA to a portion of the purified enzyme−Trp-AMP complex at 4 °C.

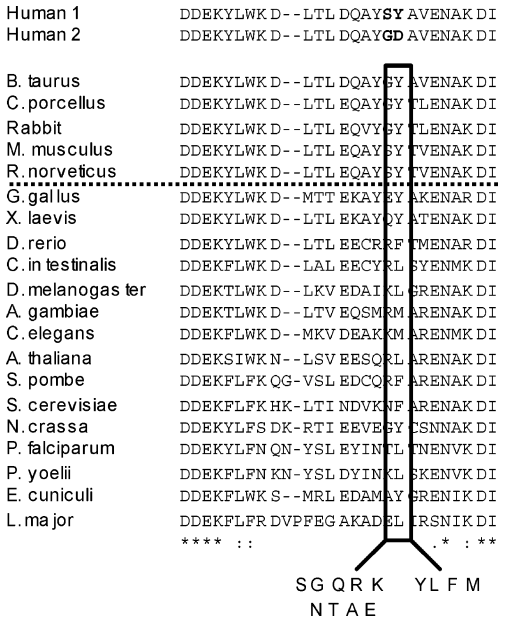

FIGURE 1: Amino acid sequence of human TrpRS (residues 197−222) deduced from a human fibroblast cDNA library varying at two adjacent positions, 213 and 214, shown in bold (*18*). Multiple sequence alignment of eukaryotic TrpRS sequences to the corresponding region in human TrpRS. Mammalian TrpRS sequences are shown above the dashed line, and other eukaryotic TrpRS sequences are below.

RESULTS

Human TrpRS Sequence Variants. The first deduced sequences of human TrpRS reported two potential polymorphic variations (*18*). The two sequences were from a human fibroblast cDNA library where two overlapping clones had nonsynonymous differences in the nucleotide sequence coding for amino acid residues 213 and 214. One sequence encoded amino acids $G^{213}D^{214}$; the other encoded $S^{213}Y^{214}$ (Figure 1) (*18*). Comparing the two sequences to five other mammalian TrpRSs, position 213 was glycine in three of five and serine in two of five sequences. Position 214 was tyrosine in all five of the other mammalian TrpRSs (Figure 1). Across eukaryotes, position 213 tolerated significant variation (S, G, A, T, E, Q, N, K, or R), whereas position 214 was restricted to large, hydrophobic amino acids (Y, L, F, or M). BLAST searches for human TrpRSs identified many mRNA and protein sequences for human TrpRS in the public databases, almost exclusively containing the SY sequence variant. Although polymorphic variants of tRNA synthetases are known (*19*, *20*), until further confirmation it remains a formal possibility that one variant (GD) was a sequence artifact. We were interested to know whether the

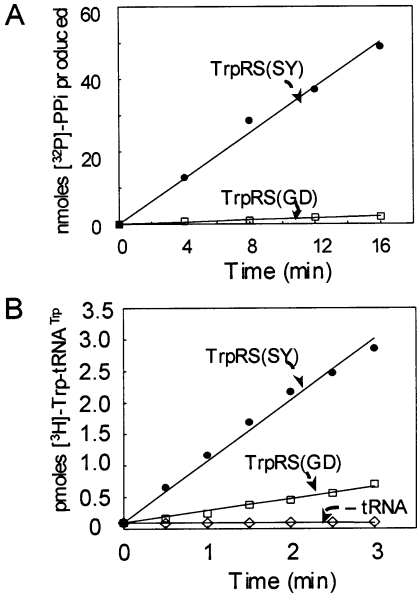

FIGURE 2: ATP−PP_i exchange and aminoacylation assays for human TrpRS sequence variants. (A) ATP−PP_i exchange catalyzed by 4 nM TrpRS. (B) [^{3}H]Tryptophan incorporation into bovine transcript $tRNA^{Trp}$ by 30 nM TrpRS. Closed circles represent TrpRS(SY), open squares represent TrpRS(GD), and diamonds are a control reaction lacking tRNA.

SY/GD variation had any effect on the enzyme and found that the variation serendipitously provided interesting mechanistic insights.

Catalytic Activity of Two Sequence Variants. Both enzymes (SY and GD variations at positions 213 and 214) were characterized in tryptophan-dependent ATP−PP_i exchange (eq 1) and aminoacylation assays (sum of eqs 1 and 2). The

$$\text{TrpRS} + \text{Trp} + \text{ATP} \leftrightarrow \text{TrpRS(Trp-AMP)} + PP_i \quad (1)$$

$$\text{TrpRS(Trp-AMP)} + \text{tRNA} \leftrightarrow \text{TrpRS} + \text{Trp-tRNA} + \text{AMP} \quad (2)$$

most frequently reported sequence variant [TrpRS(SY)] had higher enzymatic activity compared to that for TrpRS(GD). In PP_i exchange reactions, which assess the reverse of amino acid activation by measuring the incorporation of [^{32}P]PP_i into ATP (eq 1), TrpRS(SY) was active, whereas TrpRS(GD) was at least 30-fold reduced in activity (Figure 2A). In contrast, aminoacylation assays (sum of eqs 1 and 2) showed that both enzymes were functional with transcripts of bovine $tRNA^{Trp}$. Specifically, TrpRS(SY) had a 5.2-fold higher activity than TrpRS(GD) in overall aminoacylation (Figure 2B). Thus, while TrpRS(GD) has only a small diminution in aminoacylation activity relative to TrpRS(SY), it showed little activity in adenylate synthesis measured by active site titrations or ATP−PP_i exchange. To pursue further these differences between these two enzymes, kinetic parameters were measured for each.

Kinetic Parameters. The apparent K_M values for the various substrates in aminoacylation assays showed that K_M's for tRNA and tryptophan for the two human enzymes were similar to those reported for bovine TrpRS (*21*, *22*). K_M for $tRNA^{Trp}$ (transcript) for TrpRS(SY) was 1.3 μM with k_{cat} of 72 min^{-1} and TrpRS(GD) was 0.8 μM with k_{cat} of 22 min^{-1}. The apparent k_{cat}/K_M for TrpRS(GD) was 29.3 μM^{-1} min^{-1}, about half relative to 57.6 μM^{-1} min^{-1} for TrpRS(SY). The

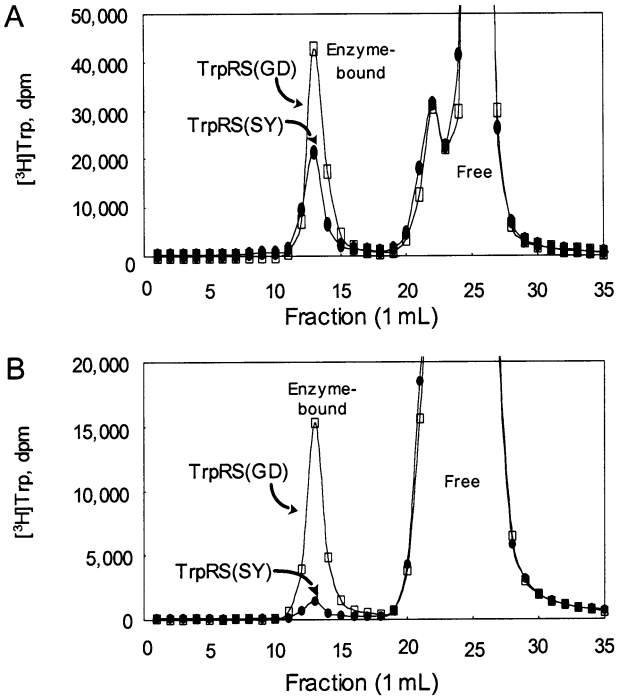

FIGURE 3: Formation of enzyme−[^{3}H]Trp-AMP complexes in the presence or absence of PP_i. TrpRS(SY) and TrpRS(GD) were incubated with [^{3}H]tryptophan and ATP in the absence of PP_i and purified by gel filtration chromatography (A). TrpRS(SY) and TrpRS(GD) were incubated with [^{3}H]tryptophan and ATP in the presence of PP_i and purified by gel filtration chromatography, and the enzyme complexes were pooled for subsequent studies (B). The amount of [^{3}H]tryptophan eluting in each fraction was measured by scintillation counting.

K_M for tryptophan was 2.5 μM [TrpRS(SY)] and 2.6 μM [TrpRS(GD)]. In contrast, the apparent K_M for ATP was about 10-fold higher for TrpRS(GD) than for TrpRS(SY) (approximately 7 versus 0.8 mM, respectively). Thus, in the aminoacylation assay, the major difference between the two enzymes was in the K_M for ATP.

Formation of the Enzyme−Trp-AMP Complex. Arginyl- and glutaminyl-tRNA synthetases do not form aminoacyl adenylate in the absence of their cognate tRNAs (*1*, *23*, *24*). Thus, we wondered whether the inability of human TrpRS-(GD) to catalyze tryptophan-dependent ATP−PP_i exchange in the absence of tRNA (eq 1) was due to the sequence variation causing a tRNA dependency for adenylate synthesis. With this in mind, we attempted to isolate complexes of Trp-AMP with both enzyme variants. Under conditions similar to the ones used in aminoacylation reactions, but in the absence of tRNA, enzyme−[^{3}H]Trp-AMP complexes were purified by gel filtration for both TrpRS(GD) and TrpRS(SY) (Figure 3A). In three separate experiments, TrpRS(GD) bound between 1.5- and 2.0-fold more [^{3}H]Trp-AMP than did TrpRS(SY) (Figure 3B). Thus, TrpRS(GD) was not defective in adenylate synthesis, nor was the amino acid activation step dependent on tRNA.

Adding 2 mM PP_i (and reducing ATP concentration accordingly from 3 to 1 mM) to drive pyrophosphorolysis and breakdown of the adenylate, we found that the TrpRS-(GD)−[^{3}H]Trp-AMP complex was formed to a greater extent than TrpRS(SY)−[^{3}H]Trp-AMP (Figure 3B). Indeed, the amount of [^{3}H]Trp-AMP bound to TrpRS(GD), under conditions of excess PP_i and lower ATP, was 10-fold higher

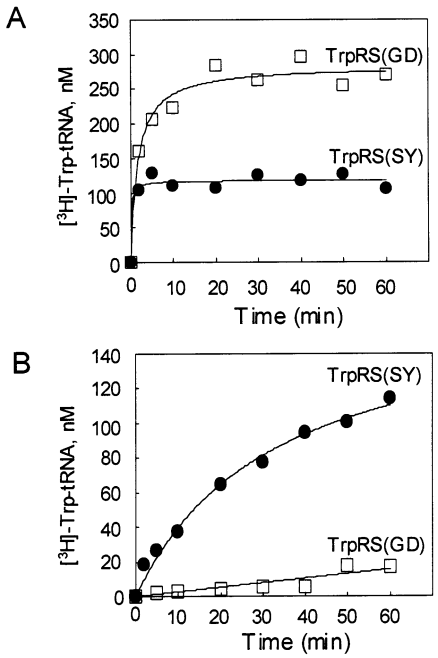

FIGURE 4: Single turnover aminoacylation of tRNA and stability of Trp-AMP bound to TrpRS(GD). Purified enzyme−[^{3}H]Trp-AMP complexes were evaluated in a single turnover reaction with 200 μM bulk yeast tRNA [300 nM enzyme (A)] or in a multiple turnover aminoacylation reaction [3 nM enzyme (B)] immediately following purification.

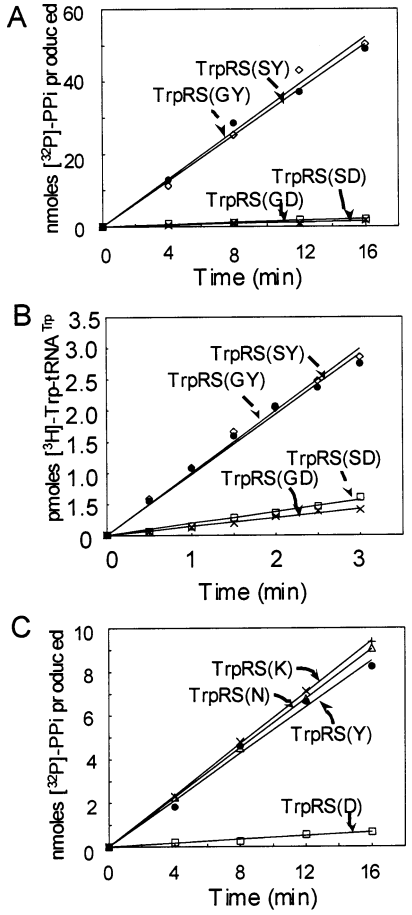

FIGURE 5: ATP−PP$_i$ exchange and aminoacylation assays for human TrpRS sequence variants at positions 213 and 214. (A) ATP−PP$_i$ exchange catalyzed by TrpRS in the presence of 10 mM PP$_i$. (B) [^{3}H]Tryptophan incorporation into bovine transcript tRNA^{Trp} by 30 nM TrpRS. In all graphs closed circles represent TrpRS(SY), open squares TrpRS(GD), open diamonds TrpRS(GY), and crosses TrpRS(SD). (C) PP$_i$ exchange assay for human TrpRS point mutants at position 214 with 2 mM PP$_i$. Closed circles represent TrpRS(Y), open squares TrpRS(D), open triangles TrpRS-(N), and crosses TrpRS(K).

than that obtained with TrpRS(SY). Collectively, the results suggest that the GD sequence variation tightly bound the aminoacyl adenylate and selectively excluded PP$_i$.

Single Turnover Reactions. To further characterize the two enzyme−adenylate complexes, each complex was purified by gel filtration and tested in single turnover reactions with tRNA. As a control, addition of hydroxylamine to the isolated complexes prevented aminoacylation of tRNA and eliminated the peak of radioactivity eluting on gel filtration as the enzyme-bound form. These results verified that the observed enzyme-bound radioactivity was [^{3}H]Trp-AMP and not free [^{3}H]Trp. To check for aminoacylation, bulk yeast tRNA was added to the enzyme−[^{3}H]Trp-AMP complexes to initiate the reactions. For both enzymes, the reaction proceeded rapidly (Figure 4A). Each reaction went to completion based on the total amount of [^{3}H]Trp isolated in the complex. The plateau level of aminoacylation for TrpRS(GD) is higher than TrpRS(SY) because TrpRS(GD) initially bound twice as much Trp-AMP.

Thus, the second step in the aminoacylation reaction (eq 2) was unaffected by the G^{213}D^{214} mutation, and the two enzymes were indistinguishable in a single turnover reaction. For internal comparison, additional [^{3}H]Trp and ATP were added to another portion of the isolated enzyme complexes in a multiple turnover reaction (Figure 4B). As was observed above in the aminoacylation reactions, TrpRS(SY) had the higher enzymatic activity. These results show that, while the GD variation excluded PP$_i$, tRNA gained free access to the reactive intermediate and was readily aminoacylated.

Identification of D214 as Important for Formation of the Trap. To elucidate the relative contributions of residues 213 and 214 to catalysis, we compared the four combinations of S/G213 and Y/D214: TrpRS(SY), TrpRS(GY), TrpRS(SD), and TrpRS(GD). Variation at position 213 (S or G) had no effect on either amino acid activation or aminoacylation activities. This observation was consistent with the presence of either S213 or G213 in sequences of mammalian TrpRS (Figure 1). However, introduction of Asp214 as a single mutation (Y214D) yielded TrpRS(SD), whose activity recapitulated that of the G^{213}D^{214} enzyme greatly reduced activity in tryptophan-dependent ATP−PP$_i$ exchange and a 7-fold decrease in aminoacylation activity (Figure 5A,B).

While eukaryotic TrpRSs contain only large hydrophobic residues at position 214, prokaryote orthologues show a broader amino acid variation at this position. We used a structure-based alignment of prokaryotic and eukaryotic TrpRSs (*6*) to identify residues homologous to position 214 in human TrpRS. The position corresponding to 214 in archeal TrpRS was occupied by large, hydrophobic amino acids (W, I, and L). Position 214 amino aicds in bacterial TrpRSs included many with different chemical properties, such as A, N, S, H, Q, R, K, L, T, Y, and F. To investigate whether position 214 in human TrpRS was inherently resistant to mutation, or whether it would accommodate mutation to residues found in prokaryotes, the site was mutated to a neutral (Y214N) and a positively charged (Y214K) residue. Significantly, both mutant enzymes were

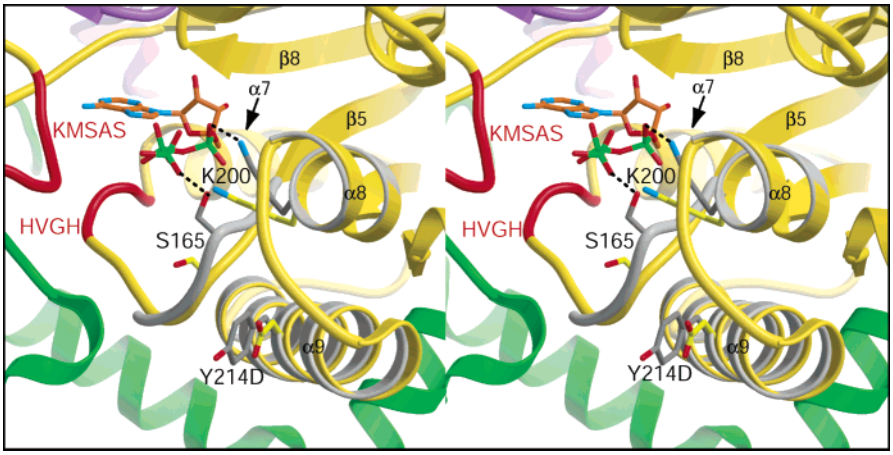

FIGURE 6: Stereoview of the human TrpRS/ATP complex model showing the structural and functional perturbation caused by the D214 mutation. The crystal structure of human TrpRS(GD) was solved with Trp-AMP bound to the dimeric enzyme. The TrpRS(GD)/Trp-AMP complex was formed during protein overexpression in *E. coli* and sustained through protein purification and crystallization. This structure was used to model the complex of human TrpRS with ATP. The TrpRS(GD) structure was color-coded (yellow, Rossmann fold domain; green, anticodon recognition domain; purple, eukaryotic-specific extension; red, KMSAS and HVGH signature sequences). Three segments with differences between the "GD" and the "GY" structures were displayed for the GY variant in gray. The Y214D mutation caused a conformational change of two residues (S165 and K200) that interact with ATP. The structural perturbation of S165 was so prominent in TrpRS(GD) that S165 was no longer able to interact with the phosphates of ATP. This structural observation is consistent with the biochemical results that GD had a 10-fold decreased affinity of ATP and diminished activity in PP_i exchange assays.

similar in their activity profiles to that of TrpRS(SY) (Figure 5C). Thus, these results show that position 214 of human TrpRS is tolerant to mutations and further support the idea that it was specifically the D214 substitution that was responsible for the altered activity.

DISCUSSION

When the crystal structures of TrpRS(GD) (PDB ID: 1R6T) and mini-TrpRS(GD) (PDB ID: 1R6U) were solved, density corresponding to Trp-AMP was found in one active site of the dimeric enzyme (in full-length TrpRS and mini-TrpRS), even though no substrate was added during crystallization. Apparently, the TrpRS(GD)/Trp-AMP complex was formed during protein overexpression in *E. coli* and sustained through protein purification and crystallization. Mini-TrpRS is an alternative splice variant lacking 47 residues at the N-terminus of full-length TrpRS. Catalytic efficiency is about the same for mini-TrpRS and full-length TrpRS, and the crystal structure of mini-TrpRS(GD) is nearly identical to that of the full-length enzyme, except for the missing N-terminal peptide. In contrast, the crystal structure of mini-TrpRS(GY) was not reported (*16*) to contain ligand. The observation that TrpRS(GD) and mini-TrpRS(GD) both trapped Trp-AMP is consistent with D214 being critical for sequestering the adenylate. Thus, during overexpression of TrpRS(GD) in *E. coli*, ATP and tryptophan were converted to Trp-AMP, but because the pyrophosphorolysis reaction is inefficient and *E. coli* $tRNA^{Trp}$ is a poor substrate for the human enzyme, the intermediate would have been trapped by TrpRS(GD) and carried through the purification. In contrast, TrpRS(SY) (gel filtration, this study) or mini-TrpRS(GY) [crystal structure (*16*)] may release Trp-AMP during production and purification from *E. coli* because the concentration of endogenous PP_i is relatively high (0.5 mM) (*25*, *26*).

Structural comparisons of mini-TrpRS(GD) and mini-TrpRS(GY) showed that the two enzymes had nearly identical overall structures, except for the bound Trp-AMP, with an rms deviation of 0.66 Å for 736 Cα atoms. Residue 214 was located on an α-helix (α9) of the Rossmann-fold domain, peripheral to the active site binding pocket. Helix α9 showed no differences between the two structures, neither D nor Y were engaged in H-bonds, and the aspartic acid and tyrosine side chains pointed in the same direction (Figure 6). However, the Y214D mutation caused an indirect conformational change between the two structures at the S165−A168 tetrapeptide that is located in the loop before the HVGH signature sequence (Figure 6). This loop and the HVGH sequence are well conserved among class I tRNA synthetases (*27*).

Although residues S165−A168 were distant from the Trp-AMP binding site, Ser165 of mini-TrpRS(GY) forms an H-bond to the γ-phosphate of ATP in the model of the mini-TrpRS/ATP complex (Figure 6). The mini-TrpRS/ATP complex model was built by taking advantage of the Trp-AMP molecule bound in the TrpRS(GD) active site and the overall similarity between the two crystal structures. S165 of human TrpRS aligns with S11 of *B. stearothermophilus* TrpRS and was involved in the same interaction with the γ-phosphate of ATP that was observed in the crystal structure of *B. stearothermophilus* TrpRS with ATP (*15*). In TrpRS-(GD), S165 is moved away from the active site and cannot interact with ATP (Figure 6). Most likely, the Y214D variation caused a local electrostatic potential change that affected the conformation of the loop where S165 is located.

In this same region of the crystal structure, K200 on helix α8 also moved. In the model of the mini-TrpRS(GY)/ATP complex, K200 interacted with the α-phosphate of ATP, whereas in the model of TrpRS(GD)/ATP, K200 had moved and no longer interacted with the α-phosphate. Instead, it shifted to interact with the γ-phosphate, possibly to compensate for the loss of S165 interaction in TrpRS(GD) (Figure 6). The movement of key residues in the phosphate binding region of the active site in the crystal structure of TrpRS-(GD) was consistent with the 10-fold decreased affinity for ATP and the strongly reduced activity in PP_i exchange

assays. Thus, structural analysis suggests a basis for how the D214 substitution excludes reaction with PP_i.

REFERENCES

1. Hong, K. W., Ibba, M., Weygand-Durasevic, I., Rogers, M. J., Thomann, H. U., and Soll, D. (1996) Transfer RNA-dependent cognate amino acid recognition by an aminoacyl-tRNA synthetase, *EMBO J. 15*, 1983−1991.
2. Wolfson, A. D., and Uhlenbeck, O. C. (2002) Modulation of tRNAAla identity by inorganic pyrophosphatase, *Proc. Natl. Acad. Sci. U.S.A. 99*, 5965−5970.
3. Cusack, S. (1995) Eleven down and nine to go, *Nat. Struct. Biol. 2*, 824−831.
4. Arnez, J. G., and Moras, D. (1997) Structural and functional considerations of the aminoacylation reaction, *Trends Biochem. Sci. 22*, 211−216.
5. Doublie, S., Bricogne, G., Gilmore, C., and Carter, C. W., Jr. (1995) Tryptophanyl-tRNA synthetase crystal structure reveals an unexpected homology to tyrosyl-tRNA synthetase, *Structure 3*, 17−31.
6. Yang, X. L., Otero, F. J., Skene, R. J., McRee, D. E., Schimmel, P., and Ribas De Pouplana, L. (2003) Crystal structures that suggest late development of genetic code components for differentiating aromatic side chains, *Proc. Natl. Acad. Sci. U.S.A. 100*, 15376−15380.
7. Ribas de Pouplana, L., Frugier, M., Quinn, C. L., and Schimmel, P. (1996) Evidence that two present-day components needed for the genetic code appeared after nucleated cells separated from eubacteria, *Proc. Natl. Acad. Sci. U.S.A. 93*, 166−170.
8. Brown, J. R., Robb, F. T., Weiss, R., and Doolittle, W. F. (1997) Evidence for the early divergence of tryptophanyl- and tyrosyl-tRNA synthetases, *J. Mol. Evol. 45*, 9−16.
9. Fersht, A. R., Leatherbarrow, R. J., and Wells, T. N. (1987) Structure−activity relationships in engineered proteins: analysis of use of binding energy by linear free energy relationships, *Biochemistry 26*, 6030−6038.
10. Fersht, A. R., Knill-Jones, J. W., Bedouelle, H., and Winter, G. (1988) Reconstruction by site-directed mutagenesis of the transition state for the activation of tyrosine by the tyrosyl-tRNA synthetase: a mobile loop envelopes the transition state in an induced-fit mechanism, *Biochemistry 27*, 1581−1587.
11. First, E. A., and Fersht, A. R. (1993) Mutational and kinetic analysis of a mobile loop in tyrosyl-tRNA synthetase, *Biochemistry 32*, 13658−13663.
12. First, E. A., and Fersht, A. R. (1993) Involvement of threonine 234 in catalysis of tyrosyl adenylate formation by tyrosyl-tRNA synthetase, *Biochemistry 32*, 13644−13650.
13. First, E. A., and Fersht, A. R. (1993) Mutation of lysine 233 to alanine introduces positive cooperativity into tyrosyl-tRNA synthetase, *Biochemistry 32*, 13651−13657.
14. First, E. A., and Fersht, A. R. (1995) Analysis of the role of the KMSKS loop in the catalytic mechanism of the tyrosyl-tRNA synthetase using multimutant cycles, *Biochemistry 34*, 5030−5043.
15. Retailleau, P., Huang, X., Yin, Y., Hu, M., Weinreb, V., Vachette, P., Vonrhein, C., Bricogne, G., Roversi, P., Ilyin, V., and Carter, C. W., Jr. (2003) Interconversion of ATP binding and conformational free energies by tryptophanyl-tRNA synthetase: structures of ATP bound to open and closed, pre-transition-state conformations, *J. Mol. Biol. 325*, 39−63.
16. Kise, Y., Lee, S. W., Park, S. G., Fukai, S., Sengoku, T., Ishii, R., Yokoyama, S., Kim, S., and Nureki, O. (2004) A short peptide insertion crucial for angiostatic activity of human tryptophanyl-tRNA synthetase, *Nat. Struct. Mol. Biol. 11*, 149−156.
17. Fersht, A. R., Ashford, J. S., Bruton, C. J., Jakes, R., Koch, G. L. E., and Hartley, B. S. (1975) Active site titration and aminoacyl adenylate binding stoichiometry of aminoacyl-tRNA synthetases, *Biochemistry 14*, 1−4.
18. Frolova, L., Sudomoina, M. A., Grigorieva, A., Zinovieva, O. L., and Kisselev, L. L. (1991) Cloning and nucleotide sequence of the structural gene encoding for human tryptophanyl-tRNA synthetase, *Gene 109*, 291−296.
19. Blechynden, L. M., Lawson, C. M., and Garlepp, M. J. (1996) Sequence and polymorphism analysis of the murine gene encoding histidyl-tRNA synthetase, *Gene 178*, 151−156.
20. Basilion, J. P., Schievella, A. R., Burns, E., Rioux, P., Olson, J. C., Monia, B. P., Lemonidis, K. M., Stanton, V. P., Jr., and Housman, D. E. (1999) Selective killing of cancer cells based on loss of heterozygosity and normal variation in the human genome: a new paradigm for anticancer drug therapy, *Mol. Pharmacol. 56*, 359−369.
21. Merle, M., Graves, P. V., and Labouesse, B. (1984) Substrate depletion analysis as an approach to the pre-steady-state anticooperative kinetics of aminoacyl adenylate formation by tryptophanyl-tRNA synthetase from beef pancreas, *Biochemistry 23*, 1716−1723.
22. Merle, M., Trezeguet, V., Gandar, J. C., and Labouesse, B. (1988) Effects of the ligands of beef tryptophanyl-tRNA synthetase on the elementary steps of the tRNA(Trp) aminoacylation, *Biochemistry 27*, 2244−2252.
23. Mehler, A. H., and Mitra, S. K. (1967) The activation of arginyl transfer ribonucleic acid synthetase by transfer ribonucleic acid, *J. Biol. Chem. 242*, 5495−5499.
24. Mitra, S. K., and Smith, C. J. (1969) Absolute requirement for transfer RNA in the activation of arginine by arginyl transfer RNA synthetase of yeast, *Biochim. Biophys. Acta 190*, 222−224.
25. Kukko, E., and Heinonen, J. (1982) The intracellular concentration of pyrophosphate in the batch culture of *Escherichia coli*, *Eur. J. Biochem. 127*, 347−349.
26. Airas, R. K. (1992) Effect of inorganic pyrophosphate on the pretransfer proofreading in the isoleucyl-tRNA synthetase from *Escherichia coli*, *Eur. J. Biochem. 210*, 451−454.
27. Webster, T., Tsai, H., Kula, M., Mackie, G. A., and Schimmel, P. (1984) Specific sequence homology and three-dimensional structure of an aminoacyl transfer RNA synthetase, *Science 226*, 1315−1317.

BI048116L